HOKKAIDO UNIVERSITY

Title	Analysis of Unamplified 16S rRNA of Ammonia-Oxidizing Bacteria in Activated Sludge by Spectrophotometry Using Gold Nanoprobes
Author(s)	Nakajima, Meri; Hirano, Reiko; Nakaya, Yuki et al.
Citation	ACS Es&t Water, 3(9), 3113-3120 https://doi.org/10.1021/acsestwater.3c00265
Issue Date	2023-09-08
Doc URL	https://hdl.handle.net/2115/92973
Rights	This document is the Accepted Manuscript version of a Published Work that appeared in final form in ACS ES&T Water, copyright © American Chemical Society after peer review and technical editing by the publisher. To access the final edited and published work see https://pubs.acs.org/articlesonrequest/AOR-WYZ9M3GIUGZB4PY8N5AN.
Type	journal article
File Information	Nakajima 2023 EST water.pdf

Hokkaido University Collection of Scholarly and Academic Papers

Hokkaido University Collection of Scholarly and Academic Papers : HUSCAP

For submission to ACS ES&T Water as a Research Article

Analysis of unamplified 16S rRNA of ammonia-oxidizing bacteria in activated sludge by spectrophotometry using gold nanoprobes

Meri Nakajima [a], *Reiko Hirano* [b], *Yuki Nakaya* [a], *Hisashi Satoh* [a,*]

[a] Division of Environmental Engineering, Faculty of Engineering, Hokkaido University, North-13, West-8, Sapporo 060-8628, Japan.

[b] Cellspect Co., Ltd., 2-4-23 Kitaiioka, Morioka, Iwate, 020-0857, Japan

Email addresses:

Meri Nakajima – meri1210@eis.hokudai.ac.jp

Reiko Hirano – hirano0317@gmail.com

Yuki Nakaya – ynakaya@eng.hokudai.ac.jp

Hisashi Satoh – qsatoh@eng.hokudai.ac.jp

ORCID

Hisashi Satoh: 0000-0002-5222-9689

Corresponding Author

*Hisashi Satoh, Division of Environmental Engineering, Faculty of Engineering, Hokkaido University, North-13, West-8, Sapporo 060-8628, Japan.

Tel: +81-(0)11-706-6277; Fax: +81-(0)11-706-6277; Email: qsatoh@eng.hokudai.ac.jp

Keywords

Simple assay; Colorimetry; PCR; Wastewater treatment; reverse transcription; heating.

Synopsis

Bacterial 16S rRNA concentration was detected colorimetrically using gold nanoparticles conjugated with DNA probe specific to target bacteria without PCR.

ABSTRACT

The identification of the bacteria contributing to the water purification processes in these systems is crucial for the development and optimization of wastewater treatment systems by engineers. We developed a simple assay for the colorimetric quantification of bacterial 16S rRNA of functional bacteria extracted from wastewater samples without reverse transcription of RNA or quantitative polymerase chain reaction (qPCR). The heat treatment of the test sample significantly reduced the reaction time (<3 min) and improved the assay sensitivity. Following assay optimization, a calibration curve for 16S rRNA of ammonia-oxidizing bacteria (AOB) of the β subdivision of the class Proteobacteria was created using 16S rRNA extracted from activated sludge samples. The curve was linear above 1.9×10^6 copies/mL of 16S rRNA of AOB, which was two orders of magnitude lower than that in our previous studies. Finally, we determined the abundance of 16S rRNA of AOB in activated sludge samples using the calibration curve and compared the results obtained by reverse transcription-qPCR. There was some correlation in the RNA concentrations of AOB determined by both methods. Thus, we have successfully developed an innovative tool to quantify the 16S rRNA concentration of AOB in wastewater treatment processes.

Graphical Abstract

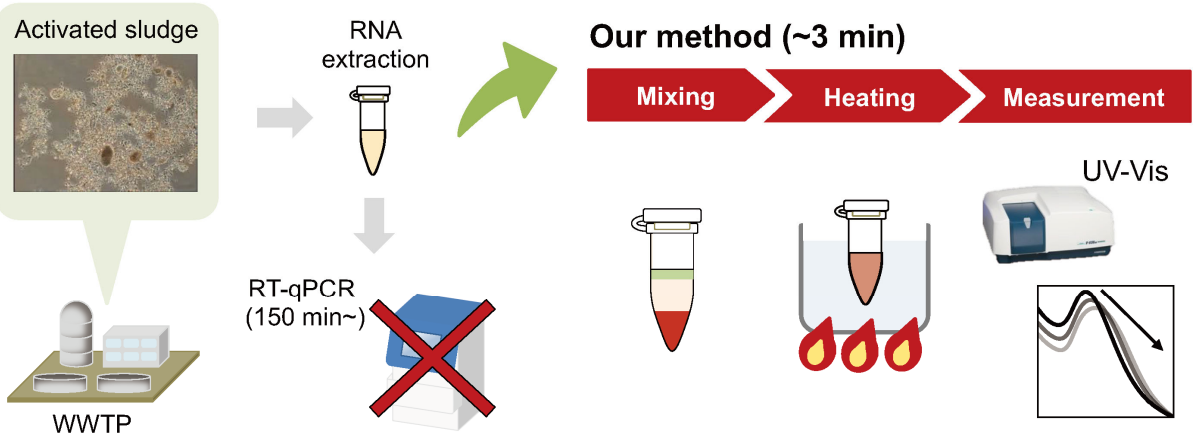

1. Introduction

Microorganisms in wastewater treatment plants (WWTPs) are essential for water purification to protect public and environmental health [1] while pathogenic ones pose serious threats to human health [2]. Rapid and accurate detection of specific target microorganisms provides many opportunities for wastewater treatment. Currently, microorganisms are analyzed using culture-dependent and culture-independent methods. Recent advances in molecular techniques have demonstrated the inadequacy of culture-dependent methodologies in unveiling the great level of diversity present in wastewater treatment systems [3,4]. Polymerase chain reaction (PCR) allows very small quantities of specific DNA sequences to be amplified with DNA polymerase, even when the target is mixed with large amounts of non-target DNA in environmental samples [5]. Unique DNA sequences are present in all microorganisms and can be used as biomarkers for their detection. Although PCR is a very powerful tool for analyzing microbial community structures and enumerating the number of specific microorganisms with extremely high sensitivity, it requires expensive enzymes (DNA polymerase) and equipment (a thermal cycler). Further, a PCR test can take several hours after a DNA extraction step and contaminants in a sample may inhibit the reaction [6]. Therefore, a low cost and rapid method for the analysis of bacterial genes in wastewater samples is required.

Another popular strategy for detecting nucleic acids is colorimetric detection. These techniques depend on the selective and specific hybridization of target strands of DNA resulting from specific Watson–Crick pairing, where a complementary DNA (probe DNA) is employed to detect whether a target is present in a sample [7,8]. AuNPs have been extensively utilized for detection of the hybridization of probe DNA to a target because AuNPs within a 5–50 nm

77 diameter range possess excellent dispersity and biocompatibility and have useful optical
78 properties derived from their surface plasmon resonance (SPR) properties [9–11]. Therefore, a key
79 step toward the establishment of an AuNP-based assay is to create an AuNP nanoprobe (Au-
80 nanoprobe). An Au-nanoprobe is generated by functionalizing AuNPs with a thiolated probe
81 DNA [12]. Hybridization of the Au-nanoprobes with a target results in the formation of the Au-
82 nanoprobe/target complex. In this case, the Au-nanoprobes are covered with a negatively charged
83 target and protected against salt-induced aggregation [13]. Therefore, they remain dispersed in the
84 solution even at a high NaCl concentration and exhibit a red color derived from the localized
85 SPR of the AuNPs. In contrast, in the absence of a target, Au-nanoprobes are not covered with
86 the target and are subjected to NaCl-induced aggregation. The aggregated An-nanoprobes exhibit
87 a red-to-blue color change based on the SPR of the AuNPs. Thus, hybridization of the Au-
88 nanoprobes with the target is detectable by colorimetric analysis [14].
89
90 In recent years, numerous AuNP-based optical biosensors have been developed for gene
91 sequence analysis [14]. Amini et al. detected the *Pseudomonas aeruginosa* exotoxin A gene using
92 AuNPs and an endonuclease enzyme [10]. A linear relationship was found between the ratio of
93 absorbance at 600 nm to 525 nm and the target DNA concentration over the range of 10–50
94 ng/mL of the target DNA with a correlation coefficient of 0.98. The optimization of the assay
95 limit of detection and limit of quantitation were reduced to be 9.9 and 34 ng/mL, respectively.
96 Baetsen-Young et al. analyzed unamplified DNA extracted from *Pseudoperonospora cubensis*,
97 the causal agent of cucurbit downy mildew [15]. They successfully detected 2.94 fM DNA and 18
98 spores/μL of *P. cubensis* using crude extracts of a pathogen matrix. These previous studies have
99 applied AuNP-based optical biosensors for clinical diagnostics and the determination of a pure

culture of a model microorganism. However, few studies have focused on the analysis of microorganisms in environmental samples [9]. We previously designed an assay for the detection of bacterial 16S rRNA using Au-nanoprobes, with 30-min detection time, without reverse transcription (RT) of RNA or qPCR [13]. The principle of our method is described as follows [13]: The format comprises using Au-nanoprobes, hybridization of targets with Au-nanoprobes, and aggregation of these. The Au-nanoprobe solutions exhibit red color and an absorbance peak of approximately 520 nm in the ultraviolet (UV)–visible spectrum. In the presence of the target, it hybridizes with the Au-nanoprobes. The Au-nanoprobes that are covered with a negatively charged target are protected against salt-induced aggregation and remain dispersed in the solution even at a high NaCl concentration. The color of the dispersed Au-nanoprobes remains red. On the other hand, in the absence of a target, Au-nanoprobes are no longer covered with a negatively charged target and protected from aggregation and, therefore, are subjected to NaCl-induced aggregation. The aggregation of AuNPs leads to a color change of AuNPs from red to blue. This process can be analyzed by UV–visible spectroscopy. Therefore, quantitative analysis of the target DNA concentration is possible by measuring the ratio of the absorbance that corresponds to the red and blue colors based on the UV–visible spectra analysis before and after the addition of NaCl. However, the limit of detection of the assay was quite high (10^8 copies/μL), and bacteria contributing to wastewater treatment (e.g., nitrification, denitrification, or phosphorous removal) could not be analyzed [16]. To the best of our knowledge, no study has determined the functional bacterial groups in a wastewater treatment process using a colorimetric assay with Au-nanoprobes.

In this study, we developed a simple assay for the direct colorimetric quantification of 16S rRNA of ammonia-oxidizing bacteria (AOB) of the β subdivision of the class Proteobacteria extracted from activated sludge (AS) samples. To detect AOB in a complex matrix, we first optimized the assay conditions, such as reaction temperature, NaCl concentration, length of a spacer molecule, and probe DNA density. After optimizing the assay protocol, we determined the abundance of 16S rRNA of AOB by the assay, and the results were compared with those determined by a qPCR method. To the best of our knowledge, this study is the first attempt to quantify the 16S rRNA of functional bacteria present in wastewater treatment processes using Au-nanoprobes. Our results have shown the feasibility of a simple colorimetric 'spot and read' test in contrast to amplification-based detection methods.

2. Materials and Methods

2.1. Chemicals and materials

Single-stranded oligonucleotides to be used as probe DNA were synthesized by Eurofins Genomics K.K. (Tokyo, Japan). Probe DNA sequences targeting the 16S rRNA of total bacteria and AOB are listed in Table 1. We designed Au-nanoprobes that are target-specific probe DNA conjugated to AuNPs. Two types of Au-nanoprobes for total bacteria were synthesized. Of the two, the probe DNA sequence for one, named 805R, was the same as the reverse PCR primer (805R, 5′-GACTACHVGGGTATCTAATCC-3′), whereas the other, named c341F, was reverse complementary to the forward PCR primer (341F, 5′- CCTACGGGNGGCWGCAG-3′) [17]. In addition, two types of Au-nanoprobes were synthesized for AOB. The probe DNA sequence for one, named RT1r, was the same as the reverse PCR primer (RT1r, 5′-CGTCCTCTCAGACCARCTACTG-3′), and the other, named cCTO 189f, was reverse

complementary to the forward PCR primer combo, CTO 189f A/B/C, which is a combination of CTO 189f A/B (5′-GGAGRAAAGCAGGGGATCG-3′) and CTO 189f C (5′-GGAGGAAAGTAGGGGATCG-3′) in a 2:1 ratio [18]. AuNPs (5 nm in diameter) in citrate buffer solution were purchased from Merck KGaA (Darmstadt, Germany, catalog number 741949). Tris(2-carboxyethyl)phosphine (TCEP) was purchased from Nacalai Tesque, Inc. (Kyoto, Japan). Sodium acetate (192−01075), acetic acid (017−00256), and sodium chloride (NaCl; 191−01665) were purchased from Fujifilm Wako Pure Chemical Corporation (Osaka, Japan). All the solutions were prepared using Milli-Q water (Merck Millipore, Tokyo, Japan).

Table 1. Sequences of probe DNA used in this study

Probe DNA	Sequence
c341F	5'HS−$(CH_2)_6$−CTGCWGCCNCCCGTAGG−3'
805R	5'HS−$(CH_2)_6$−GACTACHVGGGTATCTAATCC−3'
cCTO 189f	5'HS−$(CH_2)_6$−CGATCCCCTRCTTTYCTCC
RT1r	5'HS−$(CH_2)_6$−CGTCCTCTCAGACCARCTACTG

2.2. RNA extraction from AS samples and cDNA synthesis

AS and anaerobic sludge samples were collected from an aeration tank in WWTP-A in Sapporo City and a biogas plant of cattle manure in Hokkaido University, respectively [19]. The size, physicochemical characteristics, and operating conditions of WWTP-A have been described previously [20]. To quantify bacterial 16S rRNA by RT-qPCR, RNA was extracted from 1 mL of AS using the RNeasy Mini Kit (Qiagen, Hilden, Germany), according to the manufacturer's instructions. This sample was named as the unamplified RNA pool. The concentration of extracted RNA was determined fluorometrically using the Quant-iT™ Ribo-Green™ RNA Assay Kit (Thermo Fisher Scientific, Waltham, MA, USA). The residual DNA in the sample was

165 successfully digested using amplification grade deoxyribonuclease (DNase) I (Thermo Fisher
166 Scientific, Waltham, MA, USA). cDNA was synthesized from an aliquot of the unamplified RNA
167 pool using a PrimeScript™ RT Reagent Kit (Perfect Real Time) (Takara Bio Inc., Shiga, Japan)
168 according to the manufacturer's instructions.
169
170 *2.3. RT-qPCR*
171 The cDNA was amplified using the primer pair, 341F and 805R, for total bacteria and the
172 primer pair, CTO 189f A/B/C and RT1r, for AOB. We prepared 20 μL of the reaction mixture in a
173 96-well PCR plate by mixing 10 μL TB Green Premix Ex Taq II, 4 pmol of each primer, 0.4 μL
174 ROX reference dye II (Takara Bio Inc., Japan), 7 μL nuclease-free water, and 1 μL cDNA. For
175 standard DNA, the nucleotide sequence corresponding to the PCR-amplified region of 16S
176 rDNA was artificially synthesized and cloned into the pTAKN-2 vector by Eurofins Genomics
177 K.K. (Tokyo, Japan). The plasmid DNA was purified and its concentration was determined
178 fluorometrically. It was serially diluted from 1.0×10^8 copies/μL to 1.0×10^1 copies/μL using
179 nuclease-free water for the preparation of standard curves for the RT-qPCR assay. All reactions
180 were performed in triplicate using an Applied Biosystems 7500 Fast Real-Time PCR System
181 (Thermo Fisher Scientific, Inc., USA). The reaction conditions were as follows: initial
182 denaturation at 95 °C for 30 s, followed by 40 cycles of amplification with denaturation at 95 °C
183 for 5 s, annealing at 56 °C for 30 s, and extension at 68 °C for 30 s for bacteria. For AOB, the
184 cycling conditions were as follows: initial denaturation at 95 °C for 30 s, followed by 40 cycles
185 of amplification with denaturation at 95 °C for 30 s, annealing at 57 °C for 1 min, and extension
186 at 72 °C for 45 s. Amplification data were collected and analyzed using the Applied Biosystems
187 7500 FAST Real-Time PCR System Sequence Detection Software (version 2.0.6) (Thermo

188 Fisher Scientific Inc., California, USA). PCR efficiency (E) was calculated using the formula E =
189 $10^{-1/\text{slope}} - 1$.
190
191 *2.4. Functionalization of AuNPs with probe DNA*
192 AuNPs were individually functionalized with probe DNA as previously described [12,13].
193 Briefly, 3 μL of 10 μM thiol-modified probe DNA solution and 2.7 μL of 10 mM TCEP were
194 added to 24.3 μL of 100 mM acetate buffer (pH 5.2) to activate the thiol-modified probe DNA. A
195 20 μL aliquot of the mixture and 3 μL of 0.1 M HCl solution were added to 300 μL of the
196 original AuNP solution. The mixture was then incubated overnight at 20 °C [21]. Thereafter, the
197 Au-nanoprobe solution was vortexed vigorously for 5 s before use.
198
199 *2.5. Assay format and procedure*
200 Scheme S1 in the Supplementary Material shows the sensing mechanism of the proposed
201 method for the detection of 16S rRNA. The format comprises hybridization of target RNA with
202 Au-nanoprobes and their aggregation by NaCl. The Au-nanoprobe solution exhibits a red color
203 and an absorbance peak at approximately 530 nm in the ultraviolet-visible (UV-vis) spectrum.
204 The target RNA hybridizes with the probe DNA on the Au-nanoprobes to create negatively
205 charged complexes which are protected against salt-induced aggregation and remain dispersed in
206 the solution even at high NaCl concentrations. Therefore, the dispersed Au-nanoprobes remain
207 red. On the other hand, in the absence of a target, Au-nanoprobes are no longer covered with a
208 negatively charged target RNA, and are therefore subjected to NaCl-induced aggregation. The
209 aggregation of AuNPs leads to a color change from red to blue. This process can be analyzed by
210 UV-vis spectroscopy. Therefore, quantitative analysis of the target RNA concentration is

possible by measuring the ratio of the absorbance intensities (designated as Rs) that correspond to the red (approximately 530 nm) and blue (approximately 600 nm) colors based on UV-vis spectra analysis. This process can be visualized in solution, even with the naked eye, as a red-to-blue color change.

For the detection of bacteria, 1 μL of unamplified RNA pool and 30 μL of 5 M NaCl stock solution were added in the same order to a 20-μL mixture of the Au-nanoprobes (c341F and 805R; at a 1:1 ratio). To detect AOB, an unamplified RNA pool and NaCl stock solution were added to a 20-μL mixture of cCTO 189f and RT1r. The test solution was then heated at 95 °C for 30 s using a thermal cycler. The test sample was allowed to stand for 1 min to cool at 20 °C, and the absorbance spectrum of 50 μL of the test solution was measured in an ultraviolet transmission-type disposable cuvette (UVC−Z8.5, VIOLAMO, AS ONE Corporation, Osaka, Japan). We investigated the optimal values for several assay parameters. The ranges of the values of the investigated parameters are summarized in Table 2.

Table 2. The ranges of the values of parameters investigated in this study

Parameter	range
Incubation temperature	95 °C for 30 sec or 20 °C for 30 min
Lengths of a poly thymine (T_n) spacer	0, 25, 50, 75 and 100 bp
Mole ratios of probe DNA to AuNP	0, 0.51, 0.73, 1.10 and 1.40
NaCl concentration in stock solutions	0, 0.5, 2.0, 3.5 and 5.0 M

3. Results and discussion

3.1. Effect of heat treatment on assay performance

Figure 1 shows the typical absorbance spectra of the test solutions using Au-nanoprobes conjugated with c341F and 805R, with and without heat treatment. A typical absorbance

spectrum of an Au-nanoprobe solution for bacteria in the presence of target RNA (a positive sample abbreviated as POS) just after the addition of 5 M NaCl stock solution without heat treatment (POS-0 min in Figure 1A) showed a maximum absorbance at 529 nm with a 0.43 peak intensity. After incubation of the POS for 30 min at 20 °C (POS-30 min in Figure 1A), the peak intensity decreased to 0.36. In contrast, the maximum absorbance of the POS just after heat treatment (POS in Figure 1B) was observed at 524 nm with a 0.40 peak intensity. In comparison with the tests without heat treatment, the peak intensity of the POS with heat treatment remained unchanged for the subsequent 30 min. This might be because the rate of nucleic acid hybridization reactions increased, their efficiency was accelerated by thermal denaturation of the target RNA molecules at 95 °C, and Au-nanoprobes were stabilized. This result indicates that heat treatment stabilized the absorbance spectra. A typical absorbance spectrum of an Au-nanoprobe solution in the absence of target 16S rRNA (a negative sample abbreviated as NEG) at 30 min after the addition of 5 M of NaCl stock solution without heat treatment (NEG-30 min in Figure 1A) showed a 0.28 peak intensity at 534 nm. A typical absorbance spectrum of the NEG with heat treatment showed a 0.30 peak intensity at 568 nm just after heat treatment (NEG in Figure 1B). The difference between the peak intensities of the POS and NEG corresponds to the slope of the calibration curve, that is, the assay sensitivity. The difference in the peak intensities of the POS and NEG with and without heat treatment were 0.10 (0.40 – 0.30) and 0.08 (0.36 – 0.28), respectively. Thus, it was concluded that heat treatment increased assay sensitivity.

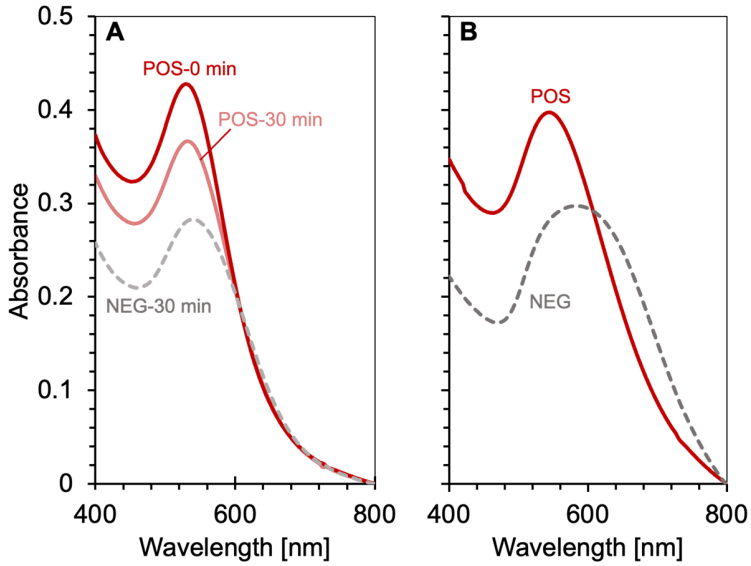

Figure 1. Typical absorbance spectra of the test solutions using Au-nanoprobes conjugated with c341F and 805R (A) without and (B) with heat treatment. The typical absorbance spectra of the Au-nanoprobe solution for bacteria in the presence of target 16S rRNA (a positive sample abbreviated as POS) just after the addition of 5 M of NaCl stock solution (POS-0 min) and after incubation of the POS for 30 min at 20 °C (POS-30 min), and the Au-nanoprobe solution in the absence of target 16S rRNA (a negative sample abbreviated as NEG) at 30 min after the addition of 5 M of NaCl stock solution (NEG-30 min) were showed in Figure 1A. The typical absorbance spectra of POS subjected to heat treatment and the corresponding NEG were showed in Figure 1B.

3.2. Effect of NaCl on assay performance

Figure 2 shows the absorbance spectra of the AuNP solution, a mixture of Au-nanoprobes conjugated with c341F and 805R, and test solutions of POS and NEG without and with NaCl and heat treatment. The absorbance spectrum of the AuNPs showed a peak at 522 nm with a 1.05 peak intensity (Figure 2A). The absorbance spectrum of the Au-nanoprobes was almost identical

to that of the AuNPs, indicating that conjugation of the probe DNA to the AuNPs did not significantly affect the absorbance spectrum. The slight decrease in the absorbance peak intensity of the Au-nanoprobes was due to dilution of the Au-nanoprobes with the buffer solution used for Au-nanoprobe preparation. The absorbance peak intensities of the POS and NEG without NaCl (POS-W and NEG-W, respectively) (Figure 2A) decreased to approximately 0.38 due to dilution of the Au-nanoprobes with the samples (an unamplified RNA pool for POS-W or nuclease-free water for NEG-W) and the buffer solution added instead of NaCl solution, but no absorbance peak shift from those of the Au-nanoprobes was observed. Since the differences in the absorbance peak intensities and their wavelengths between POS-W and NEG-W correspond to the assay sensitivity, the sensitivity of the assay without NaCl seemed to be quite low.

The absorbance peak intensities of the POS and NEG in the presence of NaCl (Figure 2B) also decreased. In this case, there was a difference between the absorbance peak intensities of the POS (0.40) and NEG (0.30), and their peak wavelengths were shifted to 544 nm and 582 nm, respectively, from those of the Au-nanoprobes (522 nm). The longer wavelength shift of the absorbance peak of AuNPs is attributed to the aggregation of AuNPs, and the SPR shifts to lower energies by the neutralization of the negative charge of AuNPs with positive Na ions [8]. The shorter absorbance peak shift for the POS-NaCl compared to the NEG-NaCl from the Au-nanoprobes might be due to the inhibition of aggregation by negatively charged RNA that hybridized to the Au-nanoprobes. These results indicated that NaCl addition was necessary for the assay and that the absorbance peak intensities of the POS and NEG can be used to determine the target RNA concentrations.

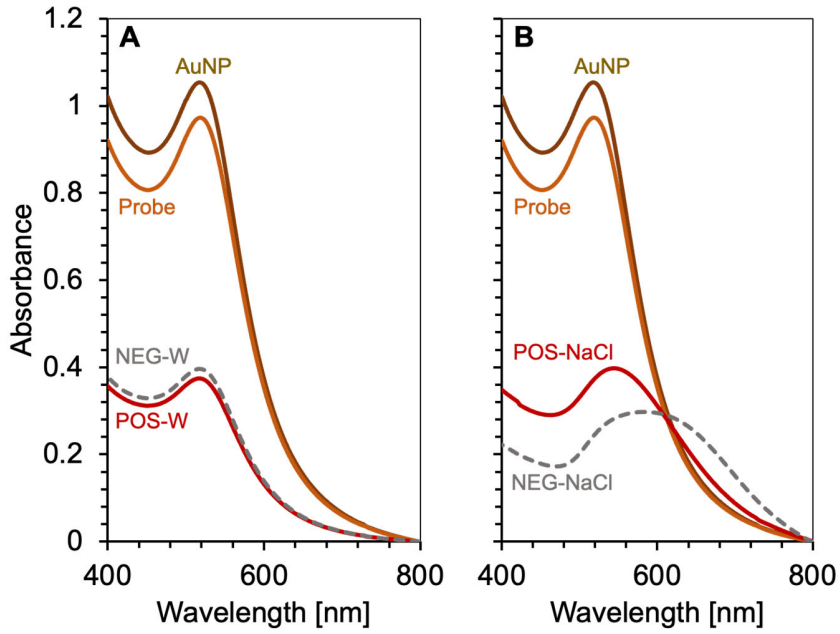

Figure 2. The absorbance spectra of test solutions (A) without and (B) with NaCl with heat treatment. The absorbance spectra of AuNPs solution (AuNP), the solution of Au-nanoprobes conjugated with c341F and 805R (Probe), the POS and NEG without NaCl (POS-W and NEG-W, respectively) were shown in Figure 2A. The absorbance spectra of AuNPs alone (AuNP), the Au-nanoprobe solution (Probe), the POS and NEG with NaCl (POS-NaCl and NEG-NaCl, respectively) were shown in Figure 2B.

3.3. Effect of the length of a spacer molecule between an AuNP and a probe DNA on assay performance

Figure S1 presented in Supplementary Material shows the absorbance spectra of the POS and NEG measured using the Au-nanoprobes conjugated with c341F and 805R with different lengths of poly(thymine) (T_n) spacers. The absorbance peak intensities of the POS were approximately 0.4 at 540 nm using the Au-nanoprobes containing T_0 to T_{75} of the T_n spacers. This result indicated that spacer length did not affect hybridization of the target RNA with the

Au-nanoprobes. The absorbance peak intensities of the NEG samples gradually increased, and their absorbance bands were shifted to shorter wavelength as the T_n spacer length increased from T_0 to T_{75}. This was because the longer spacer inhibited aggregation of the free Au-nanoprobes more significantly.

Figure S2 presented in Supplementary Material shows the effect of T_n spacer length on Rs at 630 nm to 530 nm of the POS and NEG samples which were calculated from the results shown in Figure S1. The Rs of the POS and NEG samples decreased from 0.59 to 0.42 and from 1.01 to 0.51, respectively, implying that the longer T_n spacers inhibited aggregation of the Au-nanoprobes regardless of the presence (POS) or absence (NEG) of the target RNA. This is because the longer T_n spacers cover a wider area of the Au-nanoprobe surface due to a higher deflection angle of the DNA probes [22], which makes the surface charge of the Au-nanoprobes more negative. There was no considerable decrease in the Rs for the POS samples compared with the NEG samples. It indicated that the T_n spacer length did not affect the Au-nanoprobe-target hybridization efficiency and the target RNA used in this study was long enough to inhibit Au-nanoprobes aggregation. Aggregation of the Au-nanoprobes was inhibited more by hybridization of the target RNA (POS) than in NEG samples, especially when using the Au-nanoprobes with the shorter T_n spacers. Therefore, the difference between the Rs values of the POS and NEG samples decreased with the increase in the length of T_n spacers. These results indicate that the T_n spacer length was one of the important parameters for the assay.

Figure S3 presented in the Supplementary Material shows the absorbance spectra of the NEG and POS samples as a function of the target RNA concentrations measured using the Au-

328 nanoprobes conjugated with c341F and 805R, which contain T_0, T_{25}, and T_{50} spacers. There were
329 considerable differences between the absorbance peak intensities of the POS and NEG samples.
330 As the target RNA concentrations decreased, the absorbance peak intensities decreased, and the
331 absorbance bands were shifted to longer wavelengths.
332
333 Based on these results, the relationship between the target RNA concentrations
334 determined by RT-qPCR and the Rs at 630 nm to 530 nm was evaluated (Figure S4,
335 Supplementary Material). The Rs at 5.4×10^7 copies/mL of the target RNA was similar
336 (approximately 0.45) regardless of the T_n spacer length of the Au-nanoprobes. The Rs values for
337 the Au-nanoprobes with T_0, T_{25}, and T_{50} spacers increased with a decrease in the target RNA
338 concentration. The increase in Rs was greater when using Au-nanoprobes with shorter T_n spacers
339 because the longer spacers on the Au-nanoprobes more significantly inhibited aggregation of the
340 Au-nanoprobes freely dissolved in the sample than that of the Au-nanoprobes with the shorter
341 spacers. Although the slope of the curve was steeper (i.e., assay sensitivity was higher) for the
342 Au-nanoprobes with shorter T_n spacers than that of the Au-nanoprobes with the longer spacers,
343 the Rs values for the Au-nanoprobes with a T_{50} spacer were more stable, especially at lower
344 concentrations of the target RNA than those with shorter T_n spacers. Thus, we used the Au-
345 nanoprobes with a T_{50} spacer.
346
347 *3.4. Effect of the probe DNA/AuNP ratio on assay performance*
348 Figure S5 in the Supplementary Material shows the Rs at 630 nm to 530 nm for the POS
349 and NEG samples, determined using the Au-nanoprobes conjugated with c341F and 805R, as a
350 function of the probe DNA/AuNP ratio by mole. This ratio affects the probe DNA density on the

surface of the Au-nanoprobe. Even when using the bare Au-nanoprobe without the probe DNA (*i.e.*, 0 of the probe DNA/AuNP ratio), the Rs of the POS sample was lower than that of the NEG sample because the target RNA could adsorb onto the AuNP surface and inhibit AuNP aggregation. Using the Au-nanoprobes at a 0.51 probe DNA/AuNP ratio, the Rs of both POS and NEG samples were similar to those of the bare Au-nanoprobe, indicating the probe DNA density on the Au-nanoprobe at this ratio neither had the capacity to inhibit Au-nanoprobe aggregation nor to hybridize with the target RNA. As the probe DNA density increased from 0.51 to 1.47 probe DNA/AuNP ratios, the Rs for the NEG samples decreased from 1.01 to 0.49 due to inhibition of salt-induced aggregation. In contrast, the Rs of the POS samples slightly decreased from 0.51 to 1.47 probe DNA/AuNP ratios, probably because the higher probe DNA density enabled more target RNA to be hybridized resulting in more inhibited aggregation of the Au-nanoprobes due to the more negative charge and physical blocking efficiency of the target RNA. The difference between the Rs of the POS and NEG samples were 0.31, 0.36, 0.37, 0.20, and 0.05 at 0, 0.51, 0.73, 1.10, and 1.47 probe DNA/AuNP ratios, respectively. The difference between the Rs of the POS and NEG samples was lower for the Au-nanoprobes with a higher probe DNA density because of the greater aggregation inhibition capacity of the Au-nanoprobes in the NEG samples. Since the difference between the Rs of the POS and NEG samples is the assay sensitivity, 0.73 probe DNA/AuNP ratio was the best for Au-nanoprobe preparation.

3.5. Effect of NaCl concentration on assay performance

Figure S6 presented in the Supplementary Material shows the absorbance spectra of the POS and NEG samples, determined using the Au-nanoprobes conjugated with c341F and 805R, as a function of NaCl concentrations. For the POS samples, the absorbance peaks shifted from

522 nm to 544 nm with the increase in NaCl concentrations, indicating aggregation of the Au-nanoprobe-RNA target complex. The absorbance peak shift was more significant (520 nm to 582 nm) for the NEG samples with the increase in NaCl concentrations, indicating more significant aggregation of the Au-nanoprobes. The absorbance peak intensities of the POS samples slightly increased from 0.37 to 0.40. In contrast, the peak intensities of the NEG samples decreased from 0.40 to 0.27 with increase in NaCl concentrations, and the absorbance bands were shifted to longer wavelengths and became broader.

Figure S7 in the Supplementary Material shows the effect of NaCl concentration on the Rs at 630 nm to 530 nm of the POS and NEG samples calculated from the results shown in Figure S6. The Rs of the POS and NEG samples both increased with increasing NaCl concentration, but the increase in Rs values was more significant in the NEG samples than in the POS samples. Therefore, the difference between the Rs values of the POS and NEG samples gradually increased with increasing NaCl concentration. Since the difference between the absorbance bands of the POS and NEG samples is assay sensitivity, a 5 M NaCl concentration in the stock solution was the best for the assay.

3.6. Quantification of 16S rRNA of AOB in AS samples by a novel colorimetric assay

Following the optimization of the operational parameters, a calibration curve for the 16S rRNA of bacteria extracted from AS samples was created using the Au-nanoprobes conjugated with c341F and 805R. The absorbance spectra of the Au-nanoprobes with serial dilutions of the target RNA in nuclease-free water were analyzed, and the Rs at 630 nm to 530 nm were plotted against the target RNA concentrations determined by RT-qPCR (Figure 3). When the target

concentrations were below 5.8×10^8 copies/mL, Rs were consistently high at approximately 3.2. As the target concentrations increased, Rs decreased from 3.2 to 0.2 at $>7.4\times10^8$ copies/mL of the target RNA concentrations. The slope of the calibration curve was −1.31 (Rs per unit logarithmic concentration). Rs of the samples without heat treatment ranged from 0.25 to 0.55 with a slope of −0.11 [13], indicating that heat treatment significantly improved assay sensitivity (i.e., the slope of the calibration curve).

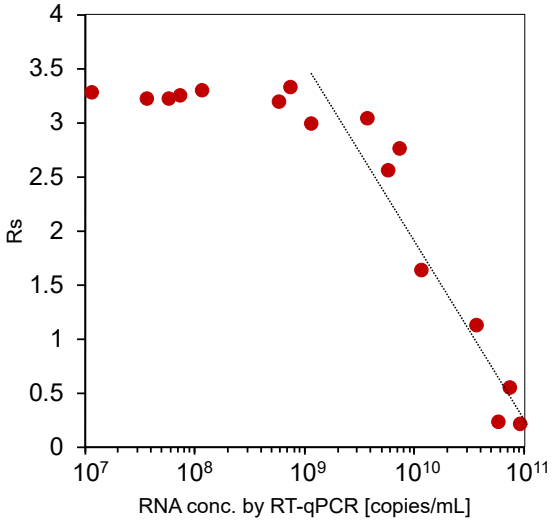

Figure 3. A calibration curve for 16S rRNA of bacteria determined by using the Au-nanoprobes conjugated with c341F and 805R created under the optimized assay conditions.

We determined the abundance of 16S rRNA of bacteria using Au-nanoprobes conjugated with c341F and 805R using the calibration curve shown in Figure 3 and compared the results with those determined by the RT-qPCR method. We extracted RNA from two AS samples and anaerobic digestion sludge samples. The 16S rRNA concentrations of bacteria ranged between 5.4×10^7 copies/mL and 4.4×10^{10} copies/mL in the unamplified RNA pools (Figure 4). There was good correlation (a determination coefficient of 0.92) between the RNA concentrations

413 determined by our method and the RNA concentrations determined by RT-qPCR at >10^8

414 copies/mL. However, the RNA concentration determined by our method overestimated the RNA

415 concentrations determined by RT-qPCR at <10^7 copies/mL. These results demonstrated that our

416 method was applicable to anaerobic sludge samples as well as aerobic AS samples.

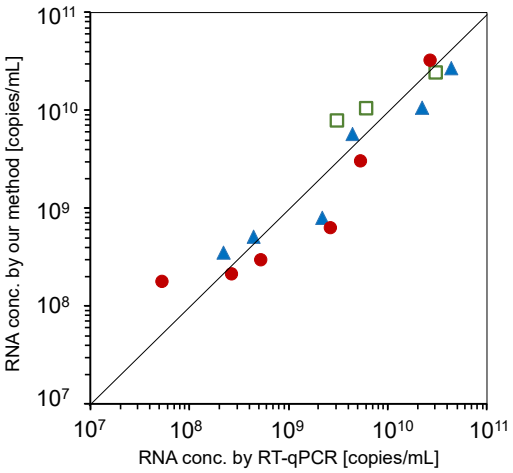

417

418 **Figure 4**. Relationship between the abundance of 16S rRNA of bacteria extracted from AS

419 samples (● and ■) and anaerobic digestion sludge samples (▲) determined by our method and

420 RT-qPCR method. The line is Y = X.

421

422 Finally, abundance of the 16S rRNA of AOB was determined by our method. A

423 calibration curve for the 16S rRNA of AOB was created using the Au-nanoprobes conjugated

424 with cCTO 189f and RT1r. The absorbance spectra of the Au-nanoprobes with serial dilutions of

425 the target RNA in nuclease-free water were analyzed, and the Rs at 630 nm to 530 nm were

426 plotted against the target RNA concentrations determined by RT-qPCR (Figure 5). When the

427 target concentrations were below 3.6×10^6 copies/mL, Rs were consistently high at approximately

428 1.2. As the target concentrations increased, Rs decreased from 1.14 to 0.48 at >9.3×10^6

429 copies/mL of the target RNA concentrations. The slope of the calibration curve was −0.66 (Rs

per unit logarithmic concentration) which was higher than that for bacteria (Figure 3). Assuming that the bacterial 16S rRNA sequence is about 1,550 bp long and the average molecular weight of a single strand RNA base is 340 Da, 10^7 copies/mL corresponded to 0.009 ng/mL. As mentioned in Introduction, 10–50 ng/mL of the target were detected in the previous reports [10]. The detection limit of our method was 4 orders of magnitude lower. This is attributed to the difference of the average molecular weight, e.g., 10^9 Da for bacterial genome and 10^5 Da for bacterial 16S rRNA.

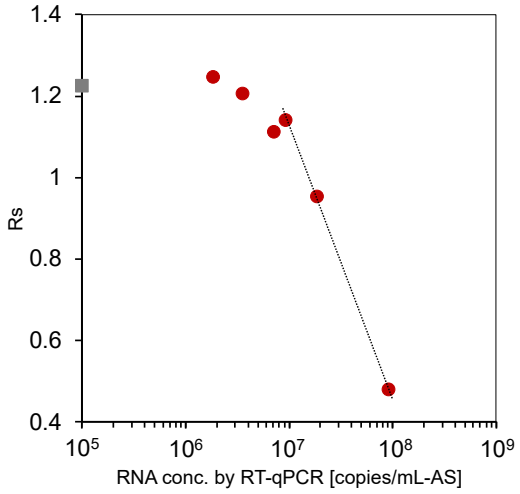

Figure 5. A calibration curve for 16S rRNA of AOB determined by using the Au-nanoprobes conjugated with cCTO 189f and RT1r created under the optimized assay conditions.

We determined the abundance of 16S rRNA of AOB using the calibration curve shown in Figure 5 and compared the results with those determined by the RT-qPCR method. We extracted RNA from the AS samples, which were incubated with an inorganic medium containing ammonium chloride in our laboratory to enrich the AOB concentrations. The 16S rRNA concentrations of AOB ranged between 9.3×10^5 copies/mL and 6.8×10^8 copies/mL in the unamplified RNA pools (Figure 6). There was some correlation between the RNA concentrations

447 determined by our method and the RNA concentrations determined by RT-qPCR in the range of
448 1.9×10^6 to 5.2×10^7 copies/mL. However, in the lower range, the RNA concentrations determined
449 by our method overestimated the RNA concentrations determined by RT-qPCR, whereas they
450 underestimated the RNA concentrations determined by RT-qPCR in the upper range.

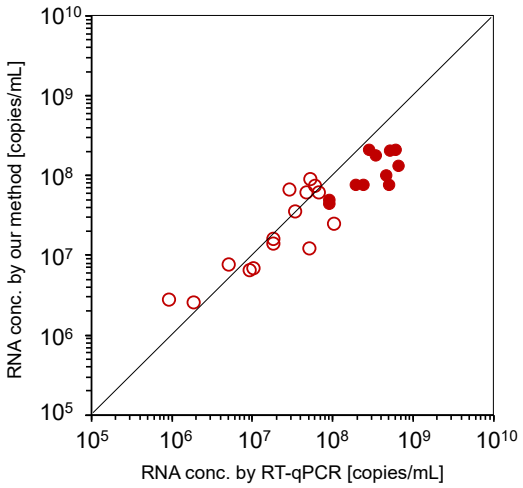

451

452 **Figure 6**. Relationship between the abundance of 16S rRNA of AOB determined by our method
453 and RT-qPCR method. Open and filled symbols indicate the samples of unamplified RNA pool
454 without and with dilution, respectively. The line is Y = X.

455

456 **4. Conclusions**

457 In this study, we developed a novel, simple assay for the quantification of unamplified
458 16S rRNA of ammonia-oxidizing bacteria in activated sludge samples. Probe DNA is an
459 oligonucleotide that hybridizes with a complementary sequence specifically present in the target.
460 When conjugated with AuNPs, it is known as an Au nanoprobe. When the Au-nanoprobes are
461 mixed with the target and NaCl solution and then heated, the Au-nanoprobes are hybridized with
462 the target and protected against salt-induced aggregation, resulting in no color change of the test
463 solution. In the absence of the target, because the Au-nanoprobes are aggregated, the test solution

exhibits a red-to-blue color change. Analysis of these absorption spectra allows for quantification of target RNA concentrations. The optimization of the assay protocol conducted in this study in terms of temperature, NaCl concentration, spacer molecule, and probe DNA density resulted in a reduction in reaction time from 30 min to <3 min and of the detection limit from 10^8 copies/mL to 10^5 copies/mL of an extraction sample, as compared with our previous study. Therefore, the assay was completed within 10 min after nucleic acid extraction. Since ammonia-oxidizing bacteria are the key players in the removal of toxic ammonia in wastewater, the assay enabling the determination of their concentration contributes to the stability and improvement of ammonia removal process in a wastewater treatment system.

Supporting Information

Scheme S1: Schematic representation of the sensing mechanism of the method for colorimetric unamplified 16S rRNA analysis. Figure S1: The absorbance spectra of test solutions without and with NaCl with heat treatment. Figure S2: The absorbance spectra of the POS and NEG samples measured using the Au-nanoprobes conjugated with c341F and 805R with T_0, T_{25}, T_{50}, and T_{75} spacers. Figure S3: The Rs of the POS and NEG samples at different length of T_n spacers. Figure S4: Typical absorbance spectra of the NEG sample and the POS samples as a function of the target RNA concentrations measured using the Au-nanoprobes containing T_0, T_{25}, and T_{50} spacers. Figure S5: Change in the Rs of the Au-nanoprobes with T_0, T_{25}, and T_{50} spacers. Figure S6: Change in the Rs of the POS and NEG samples determined by using the Au-nanoprobes conjugated with c341F and 805R as a function of the probe DNA/AuNP ratio. Figure S7: Typical absorbance spectra of the POS and NEG samples determined by using the Au-nanoprobes conjugated with c341F and 805R as a function of the NaCl concentrations in stock solutions.

Figure S8: Change in the Rs of the POS and NEG samples as a function of NaCl concentrations in stock solution. These materials are available free of charge via the internet at http://pubs.acs.org.

Acknowledgements

This research was supported financially by the JSPS KAKENHI (grant numbers 21H04568, 21H01471, 21K18737, 20KK0090, 22J21154).

CRediT authorship contribution statement

Meri Nakajima: Investigation, Formal analysis, Data curation, Validation, Writing – original draft. Reiko Hirano: Investigation, Formal analysis, Data curation, Validation. Yuki Nakaya: Conceptualization, Methodology, Validation, Supervision. Writing – review & editing. Hisashi Satoh: Conceptualization, Methodology, Validation, Supervision. Writing – review & editing.

Declaration of interests

The authors declare that they have no known competing financial interests or personal relationships that could have appeared to influence the work reported in this paper.

REFERENCES

(1) Wu, L.; Ning, D.; Zhang, B.; Li, Y.; Zhang, P.; Shan, X.; Zhang, Q.; Brown, M. R.; Li, Z.; Van Nostrand, J. D.; Ling, F.; Xiao, N.; Zhang, Y.; Vierheilig, J.; Wells, G. F.; Yang, Y.; Deng, Y.; Tu, Q.; Wang, A.; Zhang, T.; He, Z.; Keller, J.; Nielsen, P. H.; Alvarez, P. J. J.;

Criddle, C. S.; Wagner, M.; Tiedje, J. M.; He, Q.; Curtis, T. P.; Stahl, D. A.; Alvarez-Cohen, L.; Rittmann, B. E.; Wen, X.; Zhou, J.; Acevedo, D.; Agullo-Barcelo, M.; Alvarez, P. J. J.; Alvarez-Cohen, L.; Andersen, G. L.; de Araujo, J. C.; Boehnke, K. F.; Bond, P.; Bott, C. B.; Bovio, P.; Brewster, R. K.; Bux, F.; Cabezas, A.; Cabrol, L.; Chen, S.; Criddle, C. S.; Deng, Y.; Etchebehere, C.; Ford, A.; Frigon, D.; Sanabria, J.; Griffin, J. S.; Gu, A. Z.; Habagil, M.; Hale, L.; Hardeman, S. D.; Harmon, M.; Horn, H.; Hu, Z.; Jauffur, S.; Johnson, D. R.; Keller, J.; Keucken, A.; Kumari, S.; Leal, C. D.; Lebrun, L. A.; Lee, J.; Lee, M.; Lee, Z. M. P.; Li, Y.; Li, Z.; Li, M.; Li, X.; Ling, F.; Liu, Y.; Luthy, R. G.; Mendonça-Hagler, L. C.; de Menezes, F. G. R.; Meyers, A. J.; Mohebbi, A.; Nielsen, P. H.; Ning, D.; Oehmen, A.; Palmer, A.; Parameswaran, P.; Park, J.; Patsch, D.; Reginatto, V.; de los Reyes, F. L.; Rittmann, B. E.; Noyola, A.; Rossetti, S.; Shan, X.; Sidhu, J.; Sloan, W. T.; Smith, K.; de Sousa, O. V.; Stahl, D. A.; Stephens, K.; Tian, R.; Tiedje, J. M.; Tooker, N. B.; Tu, Q.; Van Nostrand, J. D.; Vasconcelos, D. D. los C.; Vierheilig, J.; Wagner, M.; Wakelin, S.; Wang, A.; Wang, B.; Weaver, J. E.; Wells, G. F.; West, S.; Wilmes, P.; Woo, S. G.; Wu, L.; Wu, J. H.; Wu, L.; Xi, C.; Xiao, N.; Xu, M.; Yan, T.; Yang, Y.; Yang, M.; Young, M.; Yue, H.; Zhang, B.; Zhang, P.; Zhang, Q.; Zhang, Y.; Zhang, T.; Zhang, Q.; Zhang, W.; Zhang, Y.; Zhou, H.; Zhou, J.; Wen, X.; Curtis, T. P.; He, Q.; He, Z.; Brown, M. R. Global Diversity and Biogeography of Bacterial Communities in Wastewater Treatment Plants. *Nature Microbiology* **2019**, *4* (7), 1183–1195.

(2) Su, J. Q.; An, X. L.; Li, B.; Chen, Q. L.; Gillings, M. R.; Chen, H.; Zhang, T.; Zhu, Y. G. Metagenomics of Urban Sewage Identifies an Extensively Shared Antibiotic Resistome in China. *Microbiome* **2017**, *5* (1), 1–15.

(3) Ferrera, I.; Sánchez, O. Insights into Microbial Diversity in Wastewater Treatment Systems: How Far Have We Come? *Biotechnology Advances* **2016**, *34* (5), 790–802.

(4) Narihiro, T.; Sekiguchi, Y. Oligonucleotide Primers, Probes and Molecular Methods for the Environmental Monitoring of Methanogenic Archaea. *Microbial Biotechnology* **2011**, *4* (5), 585–602.

(5) Jarman, S. N.; Deagle, B. E.; Gales, N. J. Group-Specific Polymerase Chain Reaction for DNA-Based Analysis of Species Diversity and Identity in Dietary Samples. *Molecular Ecology* **2004**, *13* (5), 1313–1322.

(6) Rajapaksha, P.; Elbourne, A.; Gangadoo, S.; Brown, R.; Cozzolino, D.; Chapman, J. A Review of Methods for the Detection of Pathogenic Microorganisms. *Analyst* **2019**, *144* (2), 396–411.

(7) Franco, R.; Pedrosa, P.; Carlos, F. F.; Veigas, B.; Baptista, P. V. Gold Nanoparticles for DNA/RNA-Based Diagnostics. In *Handbook of Nanoparticles*; Aliofkhazraei, M., Ed.; Springer International Publishing: Switzerland, 2016; pp 1339–1370.

(8) Nourisaeid, E.; Mousavi, A.; Arpanaei, A. Colorimetric DNA Detection of Transgenic Plants Using Gold Nanoparticles Functionalized with L-Shaped DNA Probes. *Physica E: Low-Dimensional Systems and Nanostructures* **2016**, *75*, 188–195.

(9) Quintela, I. A.; De Los Reyes, B. G.; Lin, C. S.; Wu, V. C. H. Simultaneous Colorimetric Detection of a Variety of Salmonella Spp. In Food and Environmental Samples by Optical Biosensing Using Oligonucleotide-Gold Nanoparticles. *Frontiers in Microbiology* **2019**, *10* (MAY), 1138.

(10) Amini, B.; Kamali, M.; Salouti, M.; Yaghmaei, P. Spectrophotometric, Colorimetric and Visually Detection of Pseudomonas Aeruginosa ETA Gene Based Gold Nanoparticles

DNA Probe and Endonuclease Enzyme. *Spectrochimica Acta - Part A: Molecular and Biomolecular Spectroscopy* **2018**, *199*, 421–429.

(11) Satoh, H.; Nakajima, M.; Hirano, R.; Nakaya, Y. Highly Sensitive and Homogeneous Detection of Unamplified RNA Based on the Light Scattering Properties of Gold Nanoparticle Probes. *Biosensors and Bioelectronics: X* **2022**, *12*, 100249.

(12) Liu, J.; Lu, Y. Preparation of Aptamer-Linked Gold Nanoparticle Purple Aggregates for Colorimetric Sensing of Analytes. *Nature Protocols* **2006**, *1* (1), 246–252.

(13) Nakajima, M.; Hirano, R.; Okabe, S.; Satoh, H. Simple Assay for Colorimetric Quantification of Unamplified Bacterial 16S rRNA in Activated Sludge Using Gold Nanoprobes. *Chemosphere* **2021**, *263*, 128331.

(14) Pylaev, T.; Avdeeva, E.; Khlebtsov, N. Plasmonic Nanoparticles and Nucleic Acids Hybrids for Targeted Gene Delivery, Bioimaging, and Molecular Recognition. *Journal of Innovative Optical Health Sciences* **2021**, *14* (4), 2130003.

(15) Baetsen-Young, A. M.; Vasher, M.; Matta, L. L.; Colgan, P.; Alocilja, E. C.; Day, B. Direct Colorimetric Detection of Unamplified Pathogen DNA by Dextrin-Capped Gold Nanoparticles. *Biosensors and Bioelectronics* **2018**, *101* (October 2017), 29–36.

(16) Kim, Y. M.; Cho, H. U.; Lee, D. S.; Park, D.; Park, J. M. Influence of Operational Parameters on Nitrogen Removal Efficiency and Microbial Communities in a Full-Scale Activated Sludge Process. *Water Research* **2011**, *45* (17), 5785–5795.

(17) Herlemann, D. P. R.; Labrenz, M.; Jürgens, K.; Bertilsson, S.; Waniek, J. J.; Andersson, A. F. Transitions in Bacterial Communities along the 2000 Km Salinity Gradient of the Baltic Sea. *ISME Journal* **2011**, *5*, 1571–1579.

(18) Hermansson, A.; Lindgren, P. E. Quantification of Ammonia-Oxidizing Bacteria in Arable Soil by Real-Time PCR. *Applied and Environmental Microbiology* **2001**, *67* (2), 972–976.

(19) Shimahata, A. Assessment of the Potential to Adopt Biogas Plants in Hokkaido and the Environmental and Economic Benefits Based on Dairy Farmers' Willingness, Hokkaido University, 2021.

(20) Satoh, H.; Kikuchi, K.; Katayose, Y.; Tsuda, S.; Hirano, R.; Hirakata, Y.; Kitajima, M.; Ishii, S.; Oshiki, M.; Hatamoto, M.; Takahashi, M.; Okabe, S. Simple and Reliable Enumeration of Escherichia Coli Concentrations in Wastewater Samples by Measuring β-d-Glucuronidase (GUS) Activities via a Microplate Reader. *Science of The Total Environment* **2020**, *715*, 136928.

(21) Zhang, X.; Servos, M. R.; Liu, J. Instantaneous and Quantitative Functionalization of Gold Nanoparticles with Thiolated DNA Using a PH-Assisted and Surfactant-Free Route. *Journal of the American Chemical Society* **2012**, *134* (17), 7266–7269.

(22) Barchanski, A.; Hashimoto, N.; Petersen, S.; Sajti, C. L.; Barcikowski, S. Impact of Spacer and Strand Length on Oligonucleotide Conjugation to the Surface of Ligand-Free Laser-Generated Gold Nanoparticles. *Bioconjugate Chemistry* **2012**, *23* (5), 908–915.

Supplementary material

Analysis of unamplified 16S rRNA of ammonia-oxidizing bacteria in activated sludge by spectrophotometry using gold nanoprobes

Meri Nakajima [a], *Reiko Hirano* [b], *Yuki Nakaya* [a], *Hisashi Satoh* [a,*]

[a] Division of Environmental Engineering, Faculty of Engineering, Hokkaido University, North-13, West-8, Sapporo 060-8628, Japan.

[b] Cellspect Co., Ltd., 2-4-23 Kitaiioka, Morioka, Iwate, 020-0857, Japan

ORCID

Hisashi Satoh: 0000-0002-5222-9689

Corresponding Author

*Hisashi Satoh, Division of Environmental Engineering, Faculty of Engineering, Hokkaido University, North-13, West-8, Sapporo 060-8628, Japan.

Tel: +81-(0)11-706-6277; Fax: +81-(0)11-706-6277; Email: qsatoh@eng.hokudai.ac.jp

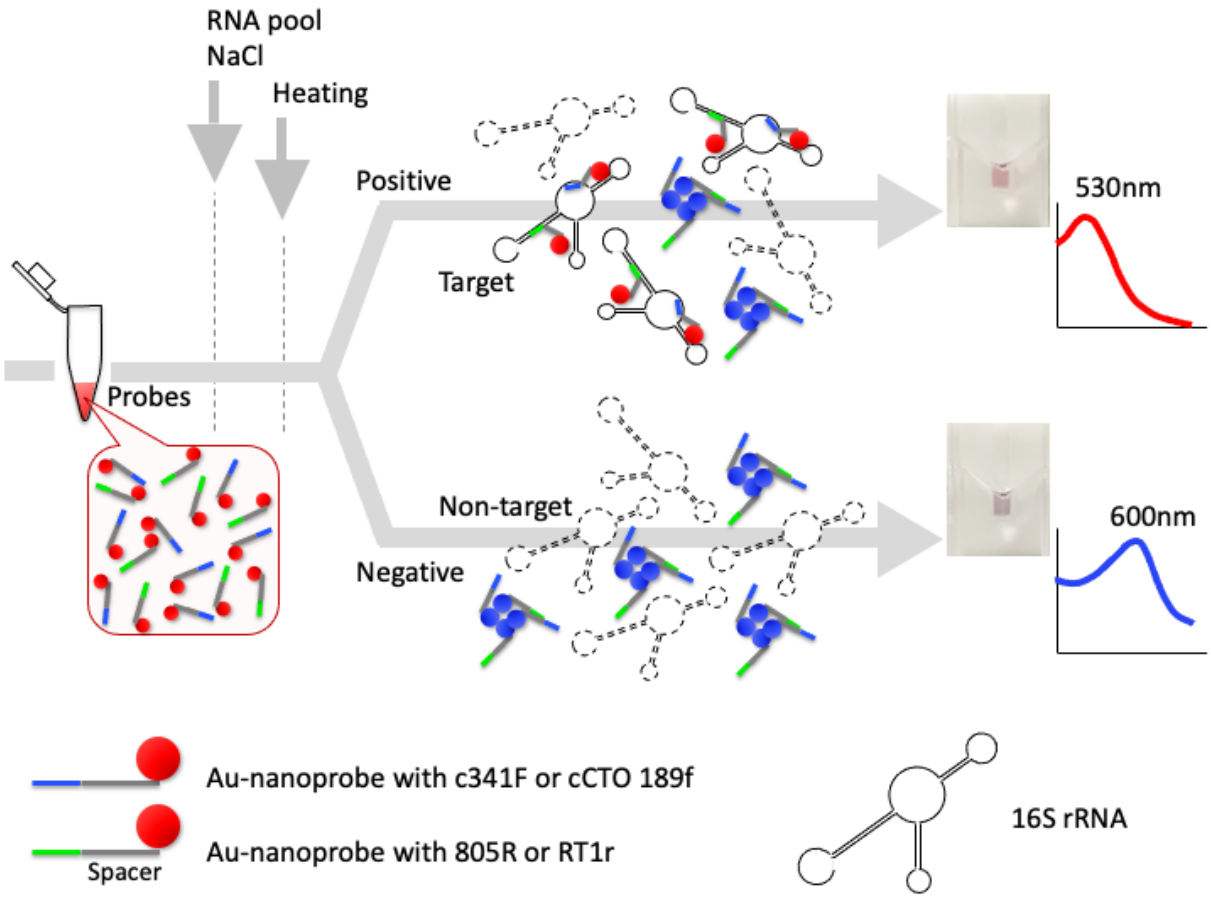

Scheme S1. Schematic representation of the sensing mechanism of the method for colorimetric unamplified 16S rRNA analysis. The Au-nanoprobes and target RNA are not drawn to scale, and 16S rRNA is believed to be much larger than depicted.

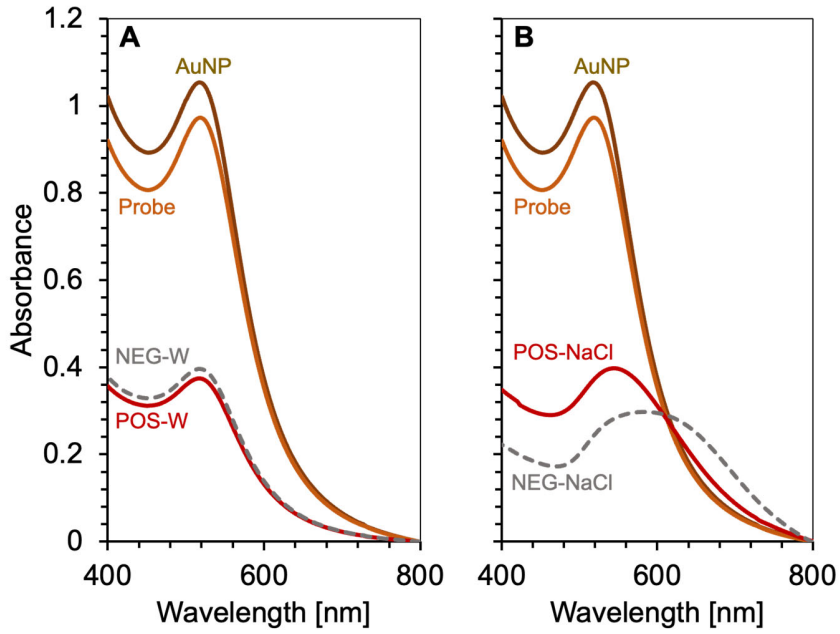

Figure S1. The absorbance spectra of test solutions (A) without and (B) with NaCl with heat treatment. The absorbance spectra of AuNPs solution (AuNP), the solution of Au-nanoprobes conjugated with c341F and 805R (Probe), the POS and NEG without NaCl (POS-W and NEG-W, respectively) were shown in Figure S1A. The absorbance spectra of AuNPs alone (AuNP), the Au-nanoprobe solution (Probe), the POS and NEG with NaCl (POS-NaCl and NEG-NaCl, respectively) were shown in Figure S1B.

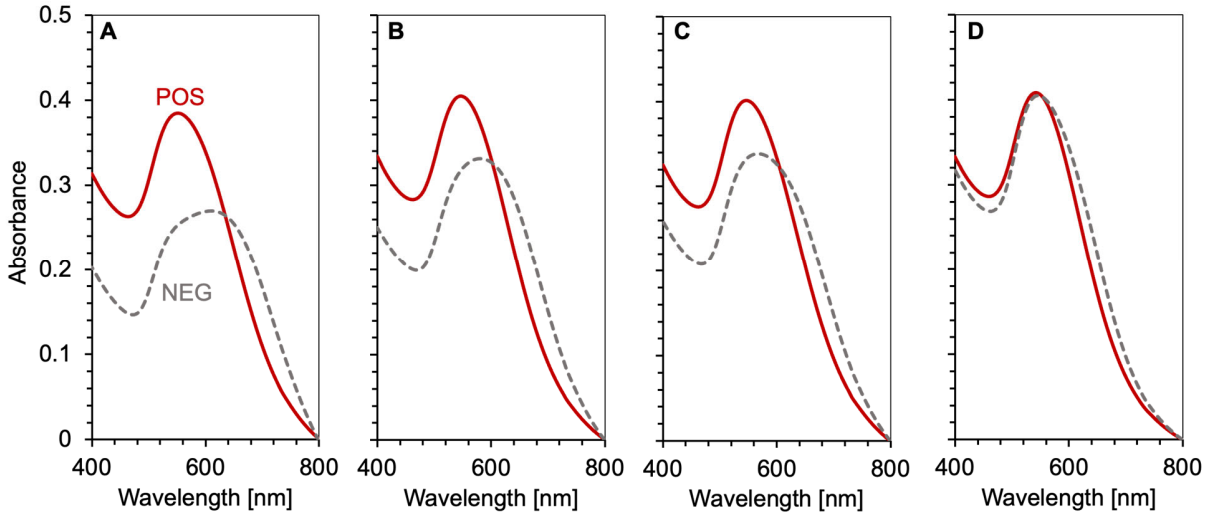

Figure S2. The absorbance spectra of the POS (a solid line) and NEG (a dashed line) samples measured using the Au-nanoprobes conjugated with c341F and 805R with (A) T_0, (B) T_{25}, (C) T_{50}, and (D) T_{75} spacers.

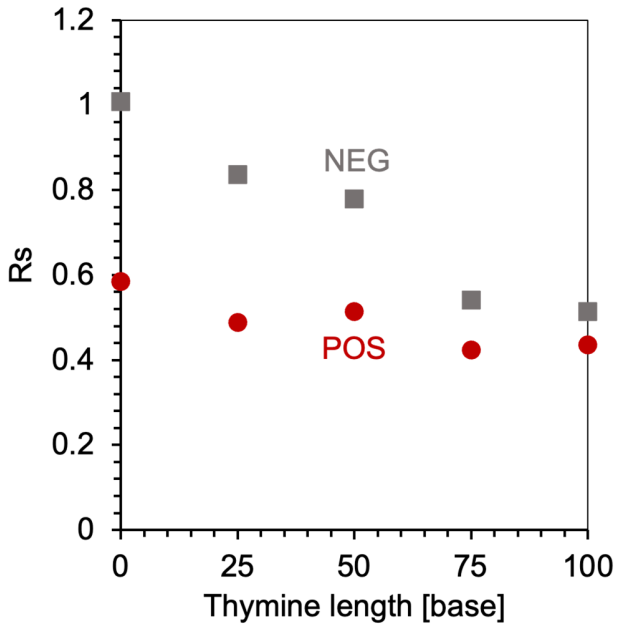

Figure S3. The Rs of the POS (●) and NEG (■) samples at different length of Tn spacers.

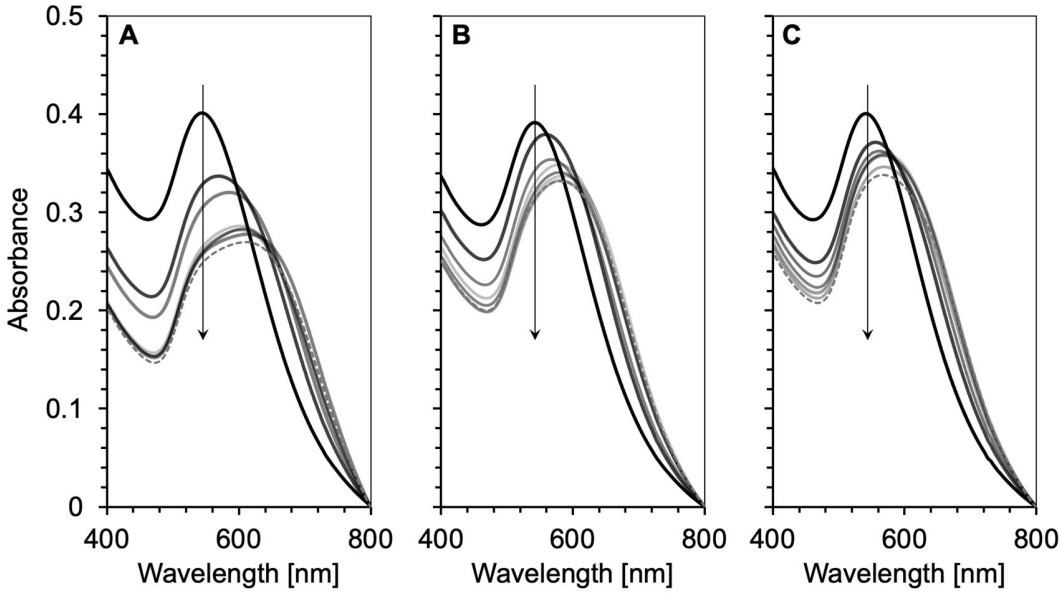

Figure S4. Typical absorbance spectra of the NEG sample (a dashed line) and the POS samples (solid lines) as a function of the target RNA concentrations (5.4×10^7 to 5.4×10^4 copies/mL) measured using the Au-nanoprobes containing (A) T_0, (B) T_{25} and (C) T_{50} spacers. The target RNA concentrations decreased from 5.4×10^7 to 5.4×10^4 copies/mL as indicated by an arrow.

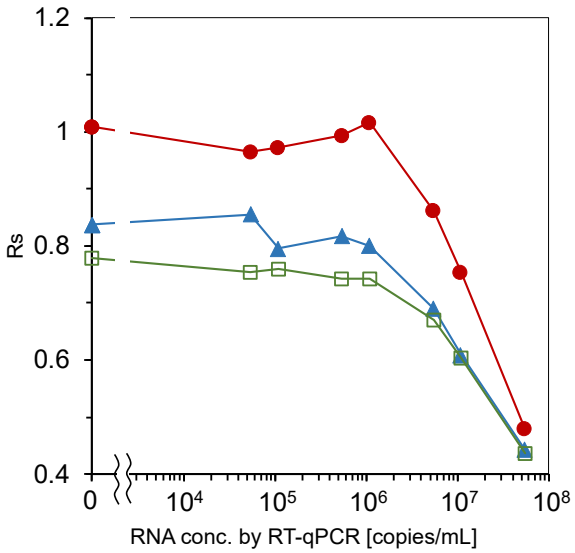

Figure S5. Change in the Rs of the Au-nanoprobes with T_0 (●), T_{25} (▲), and T_{50} (□) spacers, which were calculated from the results shown in Figure S4. The target RNA concentrations shown on the horizontal axis were determined by RT-qPCR..

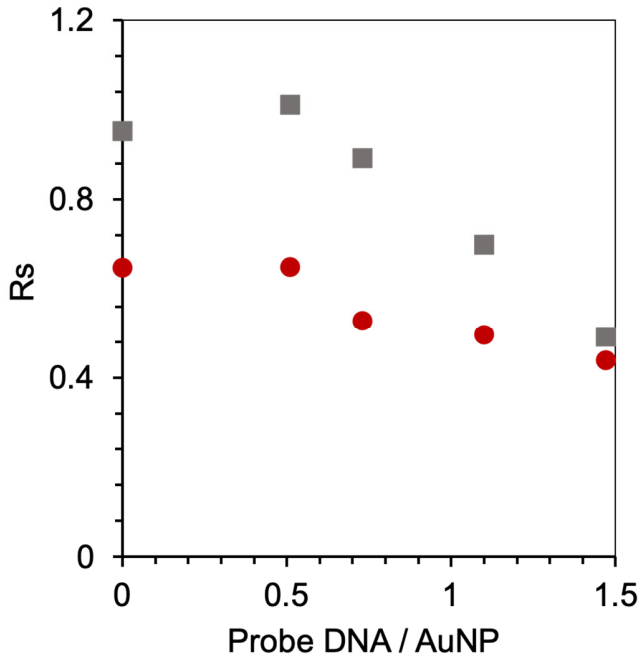

Figure S6. Change in the Rs of the POS (●) and NEG (■) samples determined by using the Au-nanoprobes conjugated with c341F and 805R as a function of the probe DNA/AuNP ratio.

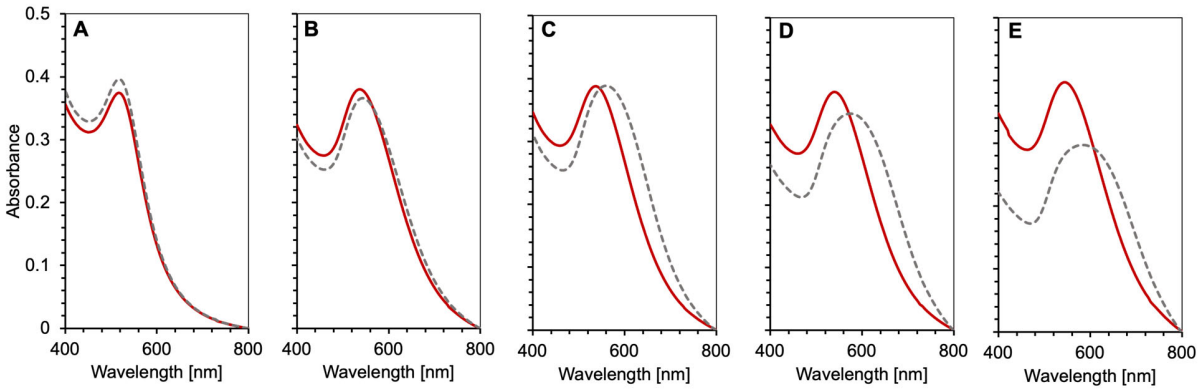

Figure S7. Typical absorbance spectra of the POS (a solid line) and NEG (a dashed line) samples determined by using the Au-nanoprobes conjugated with c341F and 805R as a function of the NaCl concentrations in stock solutions. NaCl concentrations were (A) 0 M, (B) 0.5 M, (C) 2.0 M, (D) 3.5 M, and (E) 5.0 M. The absorbance spectra were measured using the Au-nanoprobes at 0.73 of the probe DNA/AuNP ratio with T_{50} spacers.

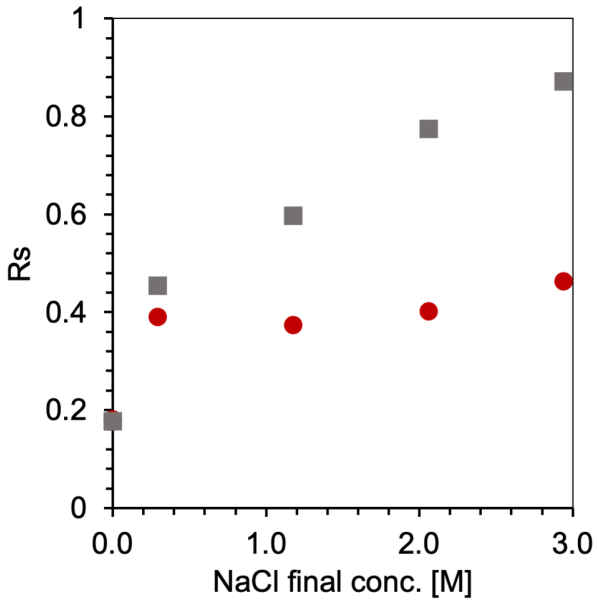

Figure S8. Change in the Rs of the POS (●) and NEG (■) samples as a function of NaCl concentrations in stock solution.